Gravitational Waves from a Fissioning White Hole

Roberto Gómez,[1, 2, *] Sascha Husa,[3, 2] Luis Lehner,[4] and Jeffrey Winicour[3, 2]

[1]*Pittsburgh Supercomputing Center, 4400 Fifth Avenue, Pittsburgh, Pennsylvania 15213*
[2]*Department of Physics and Astronomy, University of Pittsburgh, Pittsburgh, Pennsylvania 15260*
[3]*Albert Einstein Institute, Max Planck Gesellschaft, Haus 1, Am Mühlenberg, Golm, Germany*
[4]*Department of Physics and Astronomy, University of British Columbia, Vancouver, British Columbia, Canada V6T 1Z1*
(Dated: 9 May 2002)

We present a fully nonlinear calculation of the waveform of the gravitational radiation emitted in the fission of a vacuum white hole. At early times, the waveforms agree with close approximation perturbative calculations but they reveal dramatic time and angular dependence in the nonlinear regime. The results pave the way for a subsequent computation of the radiation emitted after a binary black hole merger.

I. INTRODUCTION

The omputation of gravitational radiation from the inspiral and merger of binary black holes poses a difficult boundary value problem. In the geometrically simplest and physically most natural treatment, the black holes are modeled by the gravitational collapse of a pair of stars (or other astrophysical bodies). However, this is a challenging hydrodynamic problem which requires simulating a pair of orbiting bodies for a sufficient time to verify a negligible amount of incoming radiation in the initial conditions, then following their subsequent collapse to black holes and finally computing the outgoing radiation in the exterior spacetime. Alternatively, in the purely vacuum approach, the individual black holes form from imploding gravitational waves. This avoids hydrodynamical difficulties at the expense of a globally complicated initial value problem. The imploding waves may emanate either (i) from a past singularity or (ii) from past null infinity $\mathcal{I}^-$. In case (i), the appropriate boundary condition at $\mathcal{I}^-$ is that there be no ingoing radiation but, assuming the time reversed version of cosmic censorship, the past singularity implies a white hole horizon $\mathcal{H}^-$ on which boundary data must be specified in some arbitrary manner in order to determine the exterior spacetime. In case (ii), ingoing radiation from $\mathcal{I}^-$ is present at early times when the black holes are formed but ingoing radiation must be absent at late times in order for the outgoing radiation to be unambiguously attributed to the merging black holes. In this work, we present a solution to the first stage of a new two-stage global treatment of the vacuum binary black hole problem [1, 2]. The approach, based upon characteristic evolution, has been carried out in the regime of Schwarzschild perturbations where advanced and retarded solutions of the linearized problem can be rigorously identified [3]. Computational experiments are necessary to study the applicability of the approach to the nonlinear regime.

From a time-reversed viewpoint, this first stage is equivalent to the determination of the outgoing radiation emitted from the fission of a white hole in the absence of ingoing radiation. This provides the physically correct "retarded" waveform for a white hole fission, were such events to occur in the universe. Although there is no standard astrophysical mechanism for producing white holes from a nonsingular matter distribution, white holes of primordial or quantum gravitational origin cannot be ruled out.

This fission problem has a simpler formulation as a characteristic initial value problem than the black hole merger problem. The boundary of the (conformally compactified) exterior spacetime contains two null hypersurfaces where boundary conditions must be satisfied: past null infinity $\mathcal{I}^-$, where the incoming radiation must vanish, and the white hole event horizon $\mathcal{H}^-$, which must describe a white hole, which is initially in equilibrium with no ingoing radiation and then distorts and ultimately fissions into two white holes with the emission of outgoing gravitational waves. If we approximate $\mathcal{I}^-$ by an outgoing null hypersurface J^-, which intersects $\mathcal{H}^-$ at an early time (approximating past time infinity i^-) close to the initial equilibrium of the white hole, then data on these two null hypersurfaces, $\mathcal{H}^-$ and J^-, constitute a standard double-null initial value problem, whose evolution determines a portion of the exterior spacetime extending to $\mathcal{I}^+$, where the outgoing radiation is computed. In contrast, the corresponding problem for the "retarded" waveform from a black hole merger involves two disjoint null hypersurfaces where boundary conditions must be satisfied: past null infinity $\mathcal{I}^-$, where the incoming radiation must vanish, and the future event horizon $\mathcal{H}^+$, which describes the merger of the two black holes and their subsequent approach to equilibrium.

In previous work [2], we treated the fission problem in the close approximation [4] as a perturbation of a Schwarzschild background. In this paper we present a

*Electronic address: gomez@psc.edu

fully nonlinear treatment that reveals new and interesting strong field behavior. We carry out the evolution of this vacuum double-null problem by means of a characteristic evolution code [5, 6, 7], using a recent version of the code which improves accuracy in the highly nonlinear region [8]. Caustics in the ingoing null hypersurfaces used to foliate the exterior spacetime restrict the evolution to the pre-fission stage.

We use a conformal horizon model [9, 10, 11] to supply the necessary null data for a horizon corresponding to a white hole fission. The conformal horizon model provides a stand-alone description of the intrinsic null geometry of the horizon. The algorithm for generating horizon data is constructed to handle a general event horizon representing the fission of a spinning white hole into two outspiraling white holes of non-equal mass [11]. The specific application in this paper is to the axisymmetric head-on fission into equal mass white holes. (The necessary data and evolution codes are, however, *not* limited to the axial symmetry of a head-on collision.) The resulting horizon geometry is an upside-down version of the standard trousers-shaped event horizon for a binary black hole merger in the time-reversed scenario.

We study a range of models extending from the perturbative close limit, in which the fission occurs in the infinite future, to the highly nonlinear regime. Nontrivial global changes, accompanied by dramatic time dependence of the horizon geometry, arise in passing from the perturbative to the highly nonlinear regime [11]. The existence of a marginally trapped surface divides the horizon into interior and exterior regions, analogous to the division of the Schwarzschild horizon by the $r = 2M$ bifurcation sphere. In passing from the perturbative to the strongly nonlinear regime there is a transition in which the fission occurs in the portion of the horizon visible from $\mathcal{I}^+$. Thus these results reveal two classes of binary white hole spacetimes, depending upon whether the crotch in the trousers (where the fission occurs) is bare, in the sense that it is visible from $\mathcal{I}^+$, or hidden inside a marginally trapped surface. In this paper we evolve this data using the characteristic code to study the properties of the gravitational radiation produced by this dramatic behavior of a white hole fission.

In Secs. II and III we review the formalism and data necessary for a characteristic evolution of the spacetime exterior to a dynamic white hole by means of the characteristic code. In Sec. IV we present the detailed waveforms for a one-parameter family of spacetimes varying from the close approximation to the highly nonlinear regime in which the fission is visible from $\mathcal{I}^+$.

We retain the conventions of our previous papers [5, 6, 7, 9, 10], with only minor changes where noted in the text. For brevity, we use the notation $f_{,x} = \partial_x f$ to denote partial derivatives and $\dot{f} = \partial_u f$ to denote retarded time derivatives. We represent tensor fields on the sphere as spin-weighted variables [12] in terms of a dyad q_A for the unit sphere metric $q_{AB} = q_{(A}q_{B)}$ in some standard choice of spherical coordinates, e.g. $x^A = (\theta, \phi)$. (The numer-

ical code uses two overlapping stereographic coordinate patches.) We compute angular derivatives of tensor fields in terms of $\eth$ and $\bar{\eth}$ operators [13], e.g. $f_{,A} = \Re(\bar{q}_A \eth f)$, to compute the gradient of a spin-weight zero (scalar) field f in terms of the spin-weight 1 field $\eth f$ and the spin-weight -1 field $\bar{\eth} f$.

II. THE DOUBLE-NULL PROBLEM FOR A FISSIONING WHITE HOLE

We treat the fission of a white hole by a double null initial value problem based upon the white hole horizon $\mathcal{H}^-$ and on an outgoing null hypersurface $\mathcal{J}^-$, which emanates from an early time slice $\mathcal{S}^-$ of $\mathcal{H}^-$ approximating the initial equilibrium of the white hole. The horizon pinches off in the future where its generators either caustic or cross, producing the (upside-down) trousers picture of a fissioning white hole.

The double-null problem, first formulated by Sachs [14], is most conveniently described in Sachs coordinates consisting of (i) an affine null parameter u along the generators of $\mathcal{H}^-$, which foliates $\mathcal{H}^-$ into cross sections $\mathcal{S}_u$ and labels the corresponding outgoing null hypersurfaces $\mathcal{J}_u$ emanating from the foliation, (ii) angular coordinates x^A which are constant both along the generators of $\mathcal{H}^-$ and along the outgoing null rays of $\mathcal{J}_u$, and (iii) an affine parameter λ along the outgoing rays normalized by $\nabla^\alpha u \nabla_\alpha \lambda = -1$, with $\lambda = 0$ on $\mathcal{H}^-$. In these $x^\alpha = (u, \lambda, x^A)$ Sachs coordinates, the metric takes the form

$$\begin{aligned} ds^2 &= -(W - g_{AB}W^A W^B)du^2 - 2dud\lambda \\ &- 2g_{AB}W^B dudx^A + g_{AB}dx^A dx^B \end{aligned} \quad (2.1)$$

We set $g_{AB} = r^2 h_{AB}$, where $\det(h_{AB}) = \det(q_{AB}) = q(x^A)$, with q_{AB} the unit sphere metric. We represent the conformal metric h_{AB} by the complex spin-weight 2 field $J = \frac{1}{2}h_{AB}q^A q^B$. The remaining dyad component, given by the real function $K = \frac{1}{2}h_{AB}q^A \bar{q}^B$, is fixed by the determinant condition $K^2 = 1 + J\bar{J}$.

The requirement that the horizon be null implies that $W = 0$ on $\mathcal{H}^-$. In addition, we fix the gauge freedom corresponding to the shift on $\mathcal{H}^-$ so that $n^a \partial_a = \partial_u$ is tangent to the generators, implying that $W^A = 0$ on $\mathcal{H}^-$. The choice of lapse that u is an affine parameter implies $\partial_\lambda W = 0$ on $\mathcal{H}^-$. We further fix the affine freedom by specifying $u = u_-$ on the early slice $\mathcal{S}^-$ approximating the asymptotic equilibrium of the white hole in the past. The outgoing null hypersurface $\mathcal{J}^-$ emanating from $\mathcal{S}^-$ approximates past null infinity $\mathcal{I}^-$.

The affine tangent to the generators of $\mathcal{H}^-$, $n^a \partial_a = \partial_u$ satisfies the geodesic equation $n^b \nabla_b n^a = 0$ and the hypersurface orthogonality condition $n^{[a} \nabla^b n^{c]} = 0$. Following the approach of Refs. [9, 10], we project four-dimensional tensor fields into the tangent space of $\mathcal{H}^-$ using the operator

$$P_a^b = \delta_a^b + n_a l^b, \qquad (2.2)$$

where $l_a = -\nabla_a u$.

The evolution proceeds along the outgoing null hypersurfaces $\mathcal{J}_u$ emanating from the foliation of $\mathcal{H}^-$ and extending to (compactified) $\mathcal{I}^+$. In this problem, the complete (and unconstrained) characteristic data on $\mathcal{H}^-$ are its (degenerate) intrinsic conformal metric $h_{AB}(u, x^A)$, or equivalently $J(u, x^A)$, expressed in terms of the affine parameter u. In addition, the characteristic data on $\mathcal{J}^-$ are its intrinsic conformal metric $h_{AB}(\lambda, x^A)$, or $J(\lambda, x^A)$ expressed in terms of its affine parameter λ.

The remaining data necessary to evolve the exterior spacetime consist of the intrinsic metric and extrinsic curvature of $\mathcal{S}^-$ (subject to consistency with the characteristic data) [14, 15]. This additional data consist of the surface area r, the inward expansion $\dot{r}$, the outward expansion $r_{,\lambda}$ and the twist [16]

$$\omega_a = P_a^b n^c \nabla_c l_b = (0, 0, \omega_A). \qquad (2.3)$$

(Our choice of shift implies that $\omega_u = \omega_\lambda = 0$.) The twist is an invariantly defined extrinsic curvature property of the $u = \text{const}$ cross sections of $\mathcal{H}^-$, independent of the boost freedom in the extensions of n_a and l_a subject to the normalization $n^a l_a = -1$.

We use the conformal horizon model to supply data J on $\mathcal{H}^-$ corresponding to a fissioning white hole for a sequence of models ranging from the close approximation to the highly nonlinear regime (see Sec. III). On $\mathcal{J}^-$, we set $J = 0$ to model the absence of ingoing radiation. In carrying out the evolution computationally, the first step is to propagate the data on $\mathcal{S}^-$ along the generators of $\mathcal{H}$ [17] so that it can be supplied as boundary data for the exterior characteristic evolution code.

A. Propagation equations on the horizon

Einstein's equations for the double-null problem decompose into (i) hypersurface equations intrinsic to the null hypersurfaces $\mathcal{J}_u$, which determine auxiliary metric quantities in terms of the conformal metric h_{AB}; (ii) evolution equations which determine the rate of change $\partial_u h_{AB}$ of the conformal metric of $\mathcal{J}_u$; and (iii) propagation equations which are constraints that need only be satisfied on $\mathcal{H}^-$ [14]. The Bianchi identities ensure that the propagation equations will be satisfied in the exterior spacetime as a result of the hypersurface and evolution equations. Integration of the propagation equations determines the additional horizon data necessary for the characteristic evolution.

One of the propagation equations is the ingoing Raychaudhuri equation $R_{uu} = 0$, which propagates the surface area variable r along the generators of $\mathcal{H}^-$ in terms

of initial conditions on $\mathcal{S}^-$. The value of $\dot{r}$ on $\mathcal{H}^-$ determines the convergence of the ingoing null rays. Once the intrinsic geometry J and the area coordinate r are known, the vacuum equation $R_{Au} = 0$ is used to propagate the twist $\omega = q^A \omega_A$ along the generators of $\mathcal{H}^-$. This determines ω in terms of its initial value at S^-. The $R_{AB} = 0$ vacuum equations propagate the outward expansion and shear of the foliation $\mathcal{S}_u$ along $\mathcal{H}^-$. The trace part propagates the outgoing expansion determined by $r_{,\lambda}$. The trace-free part is an evolution equation for $h_{AB,\lambda}$, which describes the shear of the outgoing rays.

In summary, the data for the double null problem include the conformal metric h_{AB} on $\mathcal{H}^-$ and $\mathcal{J}^-$ and the quantities r, $\dot{r}$, ω and $r_{,\lambda}$ on $\mathcal{S}^-$. Equations (A1), (2.29), (2.30), and (2.34) of Ref. [11] propagate the data on $\mathcal{S}^-$ to all of $\mathcal{H}^-$. The data required on $\mathcal{S}^-$ can be inferred from the asymptotic properties of the white hole equilibrium at i^-. The propagation equations, given in spin-weighted form in [11], are implemented numerically with a second order Runge-Kutta scheme [18]. Complete details can be found in Ref. [11].

B. Bondi-Sachs coordinates and characteristic code variables

The null code is based upon the Bondi-Sachs version of the characteristic initial value problem [19, 20]. It is designed to evolve forward in time along a foliation of spacetime by outgoing null hypersurfaces. The Bondi-Sachs coordinates differ from the Sachs coordinates (2.1) by the use of a surface area coordinate r along the outgoing cones rather than the affine parameter λ. Because a generic horizon is not a hypersurface of constant r, it is advantageous to first discuss the necessary data in terms of Sachs coordinates and then transform to the r coordinate. In Bondi-Sachs variables, the metric takes the form

$$ds^2 = -\left(e^{2\beta}\frac{V}{r} - r^2 h_{AB}U^A U^B\right) du^2 - 2e^{2\beta} du dr$$
$$-2r^2 h_{AB}U^B du dx^A + r^2 h_{AB} dx^A dx^B. \quad (2.4)$$

The field U^A is represented in spin-weighted form $U = q_A U^A$.

The evolution of the exterior spacetime requires a transformation of the data on $\mathcal{H}^-$ from Sachs coordinates (u, λ, x^a) to Bondi-Sachs coordinates (u, r, x^a), as described in detail in Ref. [11]. Since r is not in general constant on $\mathcal{H}^-$, the horizon does not lie precisely on radial grid points r_i. Consequently, an accurate prescription of boundary values on the r_i grid points nearest the horizon requires a Taylor expansion of the horizon data. Restricted to $\mathcal{H}^-$, the metric variables r and J have the same values in both Sachs and Bondi-Sachs coordinates and our choices of lapse and shift imply that the Bondi-Sachs variables β, U and V are related to Sachs variables by Eqs. (2.15), (2.31), and (2.32) of Ref. [11].

A similar construction [11] provides their first r derivatives in terms of known Sachs variables. We obtain $J_{,r}$ from Eq. (2.33) of Ref. [11], $\beta_{,r}$ from the $R_{\lambda\lambda} = 0$ Raychaudhuri equation for the outgoing null geodesics, Eq. (2.37) of Ref. [11], and the value of $\partial_r U$ on the horizon from the auxiliary field $Q = q^A Q_A$, where

$$Q_A = r^2 e^{-2\beta} h_{AB} U^B_{,r}. \qquad (2.5)$$

Here Q is obtained from the twist and other Sachs variables as per Eq. (2.39) of [11]. Finally, we compute $\partial_r V$ by obtaining $V_{,\lambda}$ from the λ derivative of Eq. (2.32) of Ref. [11].

The values of each metric function (J, β, U, V) and its first radial derivative can be used to consistently initialize field values at the r_i-grid points near the horizon. Boundary values for the code are then provided, to second order accuracy, on grid points bracketing the horizon. For each outgoing null ray the value of the area coordinate $r_{\mathcal{H}^-}$ on the horizon is known. This value is bracketed by the nearest grid points $r_{i-1} \leq r_{\mathcal{H}^-} < r_i$, where the metric values are computed by the second order accurate Taylor expansion

$$J_{r_i} = J|_{\mathcal{H}^-} + (r_i - r_{\mathcal{H}^-}) J_{,r}|_{\mathcal{H}^-}. \qquad (2.6)$$

After the metric quantities have been computed at the grid points neighboring the horizon, the code can evolve the spacetime exterior to the horizon.

C. Evolution equations

The system of equations that determines the exterior spacetime forms a hierarchy [21, 22]. Alternative formulations are available; see for instance Ref. [6]. Here we use a recent formulation [8], which was specifically developed to handle the extremely nonlinear post-merger regime of binary black hole collisions. It reduces all angular derivatives to first order by introducing the auxiliary variables $\nu = \eth J$, $k = \eth K$ and $B = \eth\beta$. This results in the hierarchy of hypersurface equations and one complex evolution equation for the conformal metric function J given by Eqs. (16)–(25) of Ref. [8]. We note that the terms on the right hand side of the evolution equation, Eq. (16) of [8], have been grouped into hypersurface terms J_H which vanish for linear perturbations of a spherically symmetric spacetime and a term P_u which isolates the only nonlinear term containing a (retarded) time derivative of J. The introduction of the auxiliary variables B, ν, and k in [8] eliminates all second angular derivatives from the hypersurface and evolution equations. This leads to substantially improved numerical behavior [8] over the standard characteristic formulation [5, 6, 23, 24] in the extremely nonlinear post-merger regime of binary black hole collisions. Details are given in Ref. [8].

We retain the radial and time integration schemes of the standard characteristic formulation. The radial integration algorithm is explained in detail in Refs. [5, 6, 25, 26]. In a departure from Ref. [6], we use a three-step iterative Crank-Nicholson scheme [27] to ensure stability of the time evolution [28].

The evolution code first integrates the hypersurface equations [Eqs. (17)–(23) of [8]] on the initial null hypersurface $\mathcal{J}^-$ in the region exterior to the horizon. The evolution equation, Eq. (16) of [8] is then used to advance to the next hypersurface in the region exterior to the horizon, etc., advancing the computation of the exterior spacetime in the region from the horizon to $\mathcal{I}^+$. The evolution continues as long as the coordinate system remains well behaved.

D. The Bondi news

The Bondi news function $N(u, x^B)$ [19, 29, 30] is an invariantly defined field on $\mathcal{I}^+$ which gives the amplitude of the flux of gravitational wave energy. Its computation requires evaluation of the conformal factor Ω_{conf} necessary to compactify the spacetime in a conformal Bondi frame [31], which is an asymptotic inertial frame in which the slices of $\mathcal{I}^+$ have unit sphere geometry. Following the approach of Ref. [6], we set $\Omega_{conf} = \omega_{conf}/r$, where $\omega_{conf}(u, x^A)$ is a smooth non-vanishing field at $\mathcal{I}^+$. At the early time u_- at which we initiate the evolution, the conformal metric h_{AB} of the outgoing null hypersurface approaches the unit sphere metric q_{AB} at $\mathcal{I}^+$ so that $\omega_{conf-} = \omega_{conf}|_{u_-} = 1$. However, as the evolution proceeds, the (u, x^A) coordinates, which are naturally adapted to $\mathcal{H}^-$, become non-inertial at $\mathcal{I}^+$. This results in the time dependence

$$(\partial_u + L^A \partial_A) \log \omega_{conf} = -\frac{1}{2} D_A L^A \qquad (2.7)$$

where L^A is the asymptotic value of U^A at $\mathcal{I}^+$ [6].

In addition, a transformation to conformal Bondi coordinates (u_B, y^A) on $\mathcal{I}^+$ is necessary to determine the Bondi news

$$\mathcal{N}(u_B, y^A) = N\big(u(u_B, y^A), x^A(u_B, y^A)\big), \qquad (2.8)$$

as measured in an inertial frame. The relevant expressions are given in Sec. IV and Appendix B of Ref. [6]. Inspection of Eqs. (B1)–(B6) of Ref. [6] reveals that second angular derivatives of the conformal factor ω_{conf} enter the calculation. For improved accuracy, we remove these second derivatives by introducing [8] the auxiliary variable $\mathcal{W} = \eth\omega_{conf}$. Since ω_{conf} is defined solely on $\mathcal{I}^+$, we use the consistency relation $\mathcal{W}_{,u} = \eth\omega_{conf,u}$ to propagate $\mathcal{W}$ along the generators of $\mathcal{I}^+$, initializing it by $\mathcal{W}_- = \eth\omega_{conf-}$. We use a combination of second-order Runge-Kutta and mid-point rule schemes [8] for the time integration of Eq. (2.7).

III. NULL DATA FOR THE AXISYMMETRIC HEAD-ON FISSION

The conformal horizon model [9, 10] supplies the conformal metric h_{AB} constituting the null data for a binary black or white hole. For the case of a head-on fission of a white hole, the model is based upon the flat space null hypersurface $\mathcal{H}$ emanating from a prolate spheroid $\mathcal{S}_0$ of eccentricity ϵ and semimajor axis a, which is embedded at a constant inertial time $\hat{t} = 0$ in Minkowski space. Traced back into the past, $\mathcal{H}$ expands to an asymptotically spherical shape. Traced into the future, $\mathcal{H}$ pinches off at points where its null rays cross or at caustic points where neighboring null rays focus.

With the dyad choice $q^A = (1, i/\sin\theta)$, the intrinsic conformal metric h_{AB} of $\mathcal{H}$ as a flat space null hypersurface is determined by the spin-weight-2 field

$$
J = \frac{1}{2} q^A q^B h_{AB}(\hat{t}, x^C)
= \frac{1}{2}\left(\frac{\hat{t} - r_\theta}{\hat{t} - r_\phi}\right) - \frac{1}{2}\left(\frac{\hat{t} - r_\phi}{\hat{t} - r_\theta}\right), \quad (3.1)
$$

where r_θ and r_ϕ are the principle radii of curvature of the spheroid. The metric of the spheroid induced by its embedding in a flat space is $\hat{g}_{AB} = \hat{r}^2 h_{AB}$, where $\hat{r}^2 \sin\theta$ is the local surface area.

The white hole horizon shares the same manifold $\mathcal{H}$ and the same (degenerate) conformal metric as its Minkowski space counterpart and Eq. (3.1) provides the conformal null data for the white hole horizon in the $\hat{t}$ foliation. But the surface area and affine parametrization of the white hole horizon and its flat space counterpart differ. As a white hole horizon, $\mathcal{H}$ extends infinitely far to the past of $\mathcal{S}_0$ to an asymptotic equilibrium with finite surface area. The intrinsic metric of the white hole horizon is given by $g_{AB} = \Omega^2 \hat{g}_{AB}$, and has local surface area $r^2 \sin\theta$ where $r = \Omega\hat{r}$. The conformal factor Ω is designed to stop the expansion of the white hole in the past so that the surface area radius asymptotically hovers at a fixed value $r = R_\infty$. The conformal factor is given by [9, 10]

$$
\Omega = -R_\infty \left(\hat{u} + \frac{\sigma^2}{12(p - \hat{u})}\right)^{-1}, \quad (3.2)
$$

where p is a model parameter, $\sigma = r_\theta - r_\phi$ is the difference between the principal curvature radii, and $\hat{u}$ is a flat space affine parameter along the generators of $\mathcal{H}$ with the same scale as $\hat{t}$ but with its origin shifted along each ray by $\hat{u} = \hat{t} - \frac{1}{2}(r_\theta + r_\phi)$. For an initially Schwarzschild white hole of mass M, $R_\infty = 2M$. Smoothness of the white hole requires that the parameter $p \geq \sigma_M/\sqrt{13}$, where σ_M is the maximum value of σ attained on $\mathcal{S}_0$. (For the prolate spheroid considered here, $\sigma_M = a\epsilon$.)

Both as a flat space null hypersurface and as a white hole horizon, $\mathcal{H}$ must obey the Raychaudhuri equation,

which governs the second derivative of the surface area with respect to the affine parameter. Because the focusing power determined by their conformal geometries are the same, the Raychaudhuri equation implies

$$
\frac{1}{r}\partial_t^2 r = \frac{1}{\hat{r}}\partial_{\hat{t}}^2 \hat{r}. \quad (3.3)
$$

Consequently, the different behavior of the surface area coordinates r and $\hat{r}$ due to the conformal factor Ω implies that the affine parametrization t on the white hole horizon is related to its flat space counterpart $\hat{u}$ according to [9]

$$
\begin{aligned}
\frac{dt}{d\hat{t}} &= \frac{9}{(12\hat{u}(\hat{u} - p) - \sigma^2)^2} \\
&\times \frac{(5p + \mu - 2\hat{u})^{2(2p/\mu+1)}}{(5p - \mu - 2\hat{u})^{2(2p/\mu-1)}}, \quad (3.4)
\end{aligned}
$$

where

$$
\mu = \sqrt{13p^2 - \sigma^2} \quad (3.5)
$$

and where the affine scale is fixed by the condition $dt/d\hat{t} \to 1$ as $\hat{t} \to -\infty$. The scale of the particular affine parameter u used for the time step in the evolution code is related to t by $u = t(1 + \epsilon\cos^2\theta)^{3/2}$ (chosen so that the null data J has early time behavior of the pure spin-weight 2 quadrupole form $J \sim -\epsilon\sin^2\theta/u$).

Equation (3.4) determines the rate of deviation of a slicing adapted to an affine parameter u of the white hole horizon from the $\hat{t}$ slicing given by the Minkowski embedding. The build up of a large relative angular dependence between the u and $\hat{t}$ foliations leads to the change in topology of the fissioning white hole and the associated pair-of-pants shaped horizon. We begin our evolution at an early slice $\mathcal{S}^-$, at $u = u_-$, where the horizon is close to equilibrium as a Schwarzschild white hole. Initially, the u and $\hat{t}$ foliations behave quite similarly. The time at which nonlinear behavior becomes significant is controlled by the location of the Minkowski spheroid $\mathcal{S}_0$, at $\hat{t} = 0$, with respect to the startup slice $\mathcal{S}^-$.

IV. WAVEFORMS FROM FISSIONING WHITE HOLES

We use the characteristic code [8] to evolve the exterior spacetime of an axisymmetric, head-on white hole fission and compute the detailed waveforms for a sequence of spacetimes in the range $0 \leq \epsilon \leq 10^{-2}$, varying from the perturbative to the highly nonlinear regime. The object is to search for new gravitational wave physics resulting from the highly nonlinear behavior of a binary horizon. For that purpose, the simulations reported here were carried out on a grid of $77 \times 77 \times 137$ (stereographic patch $\times$ radial) points. At this resolution, a higher eccentricity evolution ($\epsilon \approx 10^{-2}$) requires approximately one hour on

a single Pentium II 750 Mhz processor. Since the numerical code has been demonstrated to be second order convergent, more accurate results, especially concerning late time behavior near the point of fission can be attained by increasing the numerical grid resolution. Even though the characteristic code [8] is not parallel, parameter search runs of the type described here are entirely feasible on computing clusters with the present code.

We initialize the simulations according to the specifications in Ref. [11], where the horizon geometry for this data was computed and studied. We begin the evolution at $u = u_- = -100$ with the initial mass $M_- = 100$ and conformal model parameters $\hat{t}_- = -10$ (which fixes the location of the spheroid $\mathcal{S}_0$), $a = 1$ (the semi-major axis of the spheroid) and $p = (10^{-2} + 10^{-5})/\sqrt{13}$ (just above the minimum value of p allowed by regularity of the conformal model for this range of eccentricities [11]. On $\mathcal{J}^-$ ($u = u_-$), we set $J = 0$ to model the absence of ingoing radiation in an initially Schwarzschild white hole.

The limit $\epsilon \to 0$ yields the Schwarzschild solution and small eccentricity corresponds to the close approximation where the fission takes place far in the future behind a marginally trapped surface so that it is hidden from external observers. For sufficiently small ϵ, the close approximation is valid in the entire exterior Kruskal quadrant but for large ϵ it is valid only at very early times. For large ϵ, the fission occurs in the region of spacetime visible from $\mathcal{I}^+$. For a critical value $\epsilon = \epsilon_c \approx 10^{-4}$ there is a transition between these two regimes. For $\epsilon < \epsilon_c$, the evolution terminates when the expansion of the outgoing null hypersurfaces vanishes along some ray. (In the Schwarzschild limit this occurs simultaneously on all rays on the black hole horizon.) For $\epsilon > \epsilon_c$, the evolution extends to the point of fission when $r \to 0$ on the equator of the white hole.

Figure 1 shows the time dependence of the fractional mass loss $\Delta M(u)/M_- = [M(u) - M_-]/M_-$ for a sequence of runs. A negligible amount of mass is radiated at startup, confirming that in all cases the initial geometry is very close to Scharzschild. The mass loss remains small until $u \approx -90$, near the location of $\mathcal{S}_0$ on $\mathcal{H}^-$, at which time a rapid change in $d\hat{t}/du$ occurs, and the mass loss rises sharply.

Following the sharp rise in $\Delta M/M_-$, a transient period is observed in all the curves. The largest contribution to the radiated energy comes from the last stage of the evolution. The total mass loss remains well below the 1% level until eccentricities of about $\epsilon \approx 10^{-5}$ are reached, when the total mass loss at the end of the simulation approaches 2% of the initial white hole mass.

At higher eccentricities, i.e. at $\epsilon \geq 10^{-4}$, most of the initial mass is radiated away during the later stages of the simulation. The rate of mass loss in the final stage is particularly dramatic in the cases $\epsilon > \epsilon_c$ where the fission is visible from $\mathcal{I}^+$.

Figure 2 shows again the mass loss profiles of Fig. 1, but now scaled by the relative amplitude $(\epsilon/\epsilon_0)^2$, with $\epsilon_0 = 10^{-6}$. The agreement seen clearly indicates that the
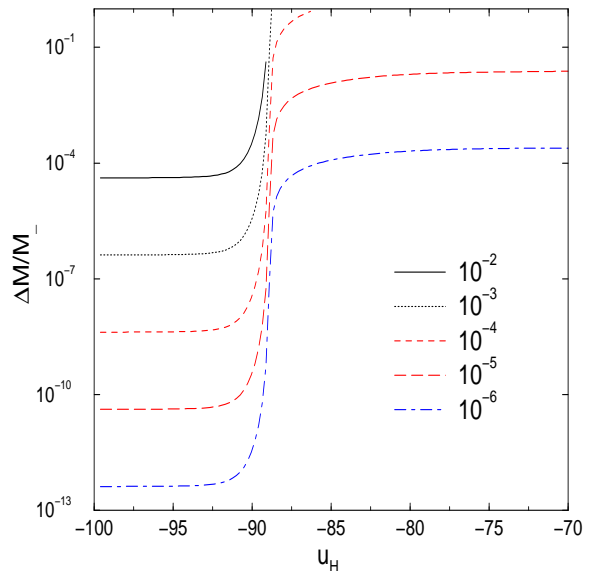

FIG. 1: Relative mass loss $\Delta M/M_0$ as a function of the horizon affine parameter u, shown here for values of the eccentricity parameter ranging from $\epsilon = 10^{-6}$ to $\epsilon = 10^{-2}$.
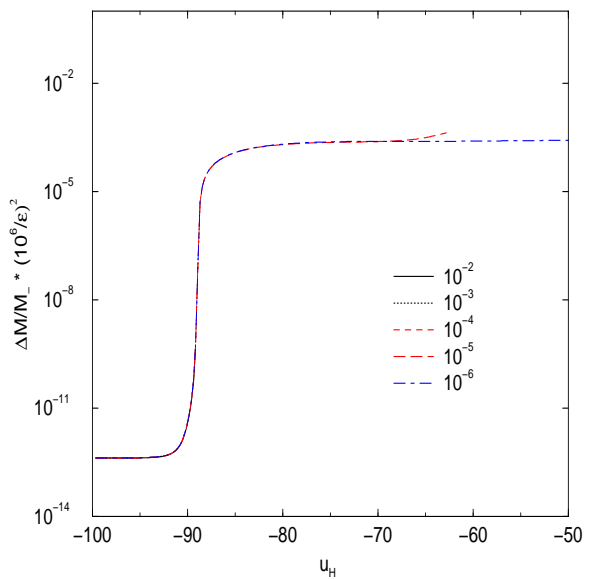

FIG. 2: The relative mass loss $\Delta M/M_0$, scaled by ϵ^2 and overlayed on the profile for the case $\epsilon = 10^{-6}$. The striking agreement indicates that the mass loss behavior is still $O(\epsilon^2)$.

behavior is $O(\epsilon^2)$ in the range where they overlap.

Figure 3 shows the time dependence of the news measured at the equator for $\epsilon = 10^{-6}$ to $\epsilon = 10^{-2}$. Here we have also overlayed the plots, rescaling them by (ϵ/ϵ_0), with $\epsilon_0 = 10^{-6}$. We plot the real part of the Bondi news at a point on the equator, as a function of Bondi time u_B. Due to axisymmetry, the imaginary part of the Bondi news is zero to within discretization error. The sharp pulse clearly visible in the news at $u_B \approx -52$ results from the choice of parameters in the white hole
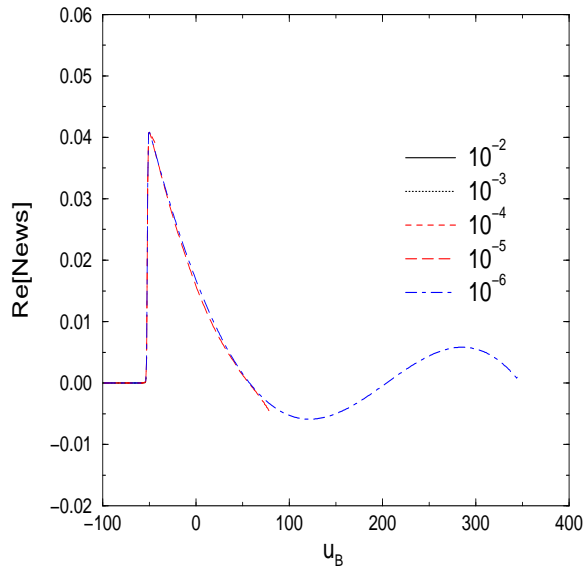
FIG. 3: The real part of the Bondi news at a point on the equator, scaled by ϵ and overlayed on the profile for the case $\epsilon = 10^{-6}$, as a function of Bondi time u_B. A sharp pulse is clearly visible at $u_B \approx -52$, which is a distinct feature of the white hole horizon data.

horizon data which control the rapidity of the fission. Here, in order that the model yield a bare fission, the parameters have been chosen so that the fission occurs on an extremely rapid time scale. Subsequent to this sharp pulse, the news undergoes a damped oscillation (which is too early in the final ringdown to be associated with a quadrupole quasinormal mode).

The Bondi news as computed by the full code osculates the results obtained in the perturbative limit [32], in the regime in which the perturbative and nonlinear codes are clearly solving the same problem (up to $u_B \approx 100$). At later times ($u_B \approx 105$), the fully nonlinear news calculation deviates from the perturbative results as a consequence of the appearance of higher harmonics. These higher harmonics, which are clearly visible in the news as a function on the sphere, arise from the nonlinearity of the equations and cannot be observed in a perturbative evolution.

Figures 4 and 5 illustrate the angular behavior of the news at early time ($u = -96.63$) and at late time ($u = -68.64$), respectively. We plot the real part of the Bondi news on a single stereographic patch for the case $\epsilon = 10^{-6}$. The graphs clearly show that at early times the news is pure quadrupole, in agreement with the perturbative regime of the close approximation. The nonlinearity of the problem subsequently introduces higher harmonics in the news. These higher harmonics are clearly visible at later times in the plots of the Bondi news as a function on the sphere. The most notable feature is the dimple seen in Fig. 5 on the profile of the news at the pole (the center of the stereographic patch).

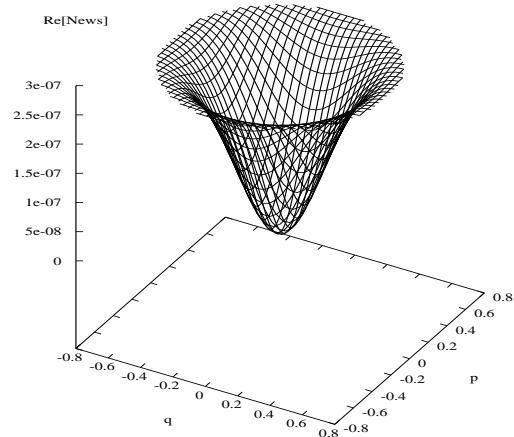This feature is partially due to the retardation effect in-

FIG. 4: The real part of the Bondi news at early times ($u = -96.63$) for $\epsilon = 10^{-6}$. At this early time, the angular dependence is purely quadrupolar.
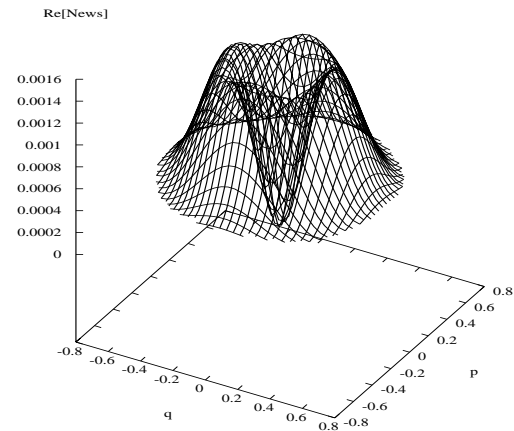

FIG. 5: The real part of the Bondi news at late times ($u = -68.64$) for $\epsilon = 10^{-6}$. The dimple visible in the angular profile is due to the presence of higher harmonics, $\ell > 2$.

troduced by the angular-dependent redshift of the Bondi frames at future null infinity $\mathcal{I}^+$. We have chosen the initial cut of $\mathcal{I}^+$, corresponding to a constant affine time u on the horizon, to be a cut of constant Bondi time. We then follow the inertial observers at $\mathcal{I}^+$ to define a Bondi time slicing. Figure 6, which displays the angular dependence of Bondi time u_B for a fixed horizon time u, reveals a pronounced increase in Bondi time at the pole relative to the equator.
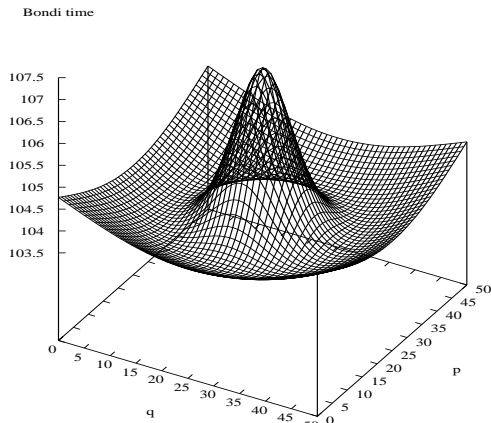
sented here are for the axisymmetric non-spinning case, the data and evolution codes are not restricted to any symmetry. It will be interesting to see how the results for a head-on collision are modified in the fission of a spinning white hole.

Reexpressed in terms of the time-reversed scenario of a black hole merger, the boundary conditions for a fission corresponds to no *outgoing* radiation in the black hole case. Nevertheless, the results pave the way for an application of characteristic codes to calculate the fully nonlinear waveform emitted in a binary black hole collision in the time period from merger to ringdown. Waveforms from a black hole merger can be expected to differ from those from a white hole fission, as has been observed in close approximation studies [3]. The fission process is directly observable at $\mathcal{I}^+$ whereas the merger waveform arises indirectly from the preceding collapse of the matter or gravitational wave energy that forms the black holes. This suggests that the fission is a more efficient source of gravitational waves and that the high fractional mass losses computed here cannot be attained in a black hole merger.

FIG. 6: The Bondi time as a function on a stereographic patch at null infinity at a late times ($u = -59.92$) for $\epsilon = 10^{-6}$. The pole is "running ahead" of the equator, leading to the dimple observed in Fig. 5.

V. CONCLUSIONS

We have computed a family of spacetimes exterior to a head-on white hole fission ranging from the close approximation to the nonlinear regime. The results reveal a dramatic time and angular dependence in the waveforms produced in the extreme nonlinear regime. At early times, the results agree with close-approximation perturbative calculations as expected. While the results pre-

Acknowledgments

[1] J. Winicour, Prog. Theor. Phys. Suppl. **136**, 57 (1999).
[2] M. Campanelli, R. Gómez, S. Husa, J. Winicour, and Y. Zlochower, Phys. Rev. D **63**, 124013 (2001).
[3] S. Husa, Y. Zlochower, R. Gómez, and J. Winicour, Phys. Rev. D **65**, 084034 (2002).
[4] R. Price and J. Pullin, Phys. Rev. Lett. **72**, 3297 (1994).
[5] Nigel T. Bishop, Roberto Gómez, Luis Lehner, and Jeffrey Winicour, Phys. Rev. D **54**, 6153 (1996).
[6] Nigel T. Bishop, Roberto Gómez, Luis Lehner, Manoj Maharaj, and Jeffrey Winicour, Phys. Rev. D **56**, 6298 (1997).
[7] R. Gómez, L. Lehner, R. L. Marsa, and J. Winicour, Phys. Rev. D **57**, 4778 (1998).
[8] Roberto Gómez, Phys. Rev. D **64**, 024007 (2001).
[9] Luis Lehner, Nigel T. Bishop, Roberto Gómez, Bela Szilágyi, and Jeffrey Winicour, Phys. Rev. D **60**, 044005 (1999).
[10] S. Husa and J. Winicour, Phys. Rev. D **60**, 084019 (1999).
[11] Roberto Gómez, Sascha Husa, and Jeffrey Winicour, Phys. Rev. D **64**, 024010 (2001).
[12] R. Penrose and W. Rindler, *Spinors and Space-Time*, (Cambridge University Press, Cambridge, England, 1984), Vol. 1.
[13] R. Gómez, L. Lehner, P. Papadopoulos, and J. Winicour, Class. Quantum Grav. **14**, 977 (1997).
[14] R. Sachs, J. Math. Phys. **3**, 908 (1962).
[15] S. A. Hayward, Class. Quantum Grav. **10**, 779 (1993).
[16] S. A. Hayward, Class. Quantum Grav. **10**, 773 (1993).
[17] R. K. Sachs, Proc. R. Soc. London **A264**, 309 (1961).
[18] W. Press, B. Flannery, S. Teukolsky, and W. Vetterling, *Numerical Recipes*, (Cambridge University Press, New York, 1986), Chap. 6.6, p. 182.
[19] H. Bondi, M. van der Burg, and A. Metzner, Proc. R. Soc. London **A269**, 21 (1962).
[20] R. Sachs, Proc. R. Soc. London **A270**, 103 (1962).
[21] J. Winicour, J. Math. Phys. **24**, 1193 (1983).
[22] J. Winicour, J. Math. Phys. **25**, 2506 (1984).
[23] Nigel T. Bishop, Roberto Gómez, Luis Lehner, Manoj Maharaj, and Jeffrey Winicour, Phys. Rev. D **60**, 024005 (1999).
[24] R. Gómez, L. Lehner, R. L. Marsa, and J. Winicour *et. al.* Phys. Rev. Lett. **80**, 3915 (1998).
[25] R. Gómez, P. Papadopoulos, and J. Winicour, J. Math.

Phys. **35**, 4184 (1994).

[26] L. Lehner, J. Comput. Phys. **149**, 59 (1999).

[27] Simonetta Frittelli and Roberto Gómez, J. Math. Phys. **41**, 5535 (2000).

[28] S. A. Teukolsky, Phys. Rev. D **61**, 087501 (2000).

[29] R. Penrose, Phys. Rev. Lett. **10**, 66 (1963).

[30] J. Winicour, *Highlights in Gravitation and Cosmology*, edited by B.R. Iyer, A. Kembhavi, J. V. Narlikar, and C.V. Vishveshwara (Cambridge University Press, Cambridge, 1988).

[31] L. Tamburino and J. Winicour, Phys. Rev. **150**, 1039 (1966).

[32] Y. Zlochower (private communication).